

# Water Budget Assessment for a Typical Watershed in the Karak Plateau, Jordan

Ibrahim M. Oroud\*

*Mu'tah University, Karak, Jordan*

*Received 14 June, 2014; Accepted 12 August, 2015*

## Abstract

Adequate assessment of water resources in arid and semiarid watersheds is essential for several purposes, such as the evaluation of biotic potentials for agricultural and grazing practices and for designing water dams. The water balance components of the watersheds in these environments are poorly understood due to the lack or the total absence of hydro-meteorological measurements. Simulation models would more likely fill this gap and can be applied to gauge these resources. The present investigation implements a physically based model with relatively fine spatial and temporal resolutions to examine the water budget components in the Numera catchment, a typical medium sized watershed draining the southwestern parts of the Karak Plateau.

The model was able to reproduce the energy balance components adequately, and the results compared favorably well with the observed data. Simulated results of the various water budget components are comparable to those obtained in similar environments. The average annual blue water fluxes (surface runoff and deep recharge) in this catchment is calculated to be ~ 3.3 million m<sup>3</sup> during the simulation period, 1996/1997 through 2001/2006. Blue water fluxes are generated primarily in the highlands of the watershed where relatively ample precipitation occurs. Steep terrains with limited vegetation cover experience significant runoff, implying the production of large quantities of sediments. The substantial sediment yield from these landscapes has serious adverse consequences on water quality and the life spans of dams constructed over these watersheds. It is imperative, therefore, that the sediment control via watershed management e.g., terracing, grazing control, preservation of native plants) be specified as a mandatory measure before constructing any dams over these watersheds.

© 2015 Jordan Journal of Earth and Environmental Sciences. All rights reserved

**Keywords:** Karak Plateau, semiarid environments, sediment control, water balance partitioning, spatial modeling.

## 1. Introduction

Being located mainly in an arid environment, Jordan suffers from chronic water problems that exacerbate further with time. The average volume of precipitation falling on the country as a whole is around 8 billion m<sup>3</sup> annually, with a value ranging from a minimum of less than 5 billion m<sup>3</sup> in very dry years to a maximum of 17 billion m<sup>3</sup> in wet years (Ministry of Water and Irrigation, 2012). The water shortage in the country will deteriorate further in the near future due to the steady growth of population resulting from natural growth and forced immigration, and also due to climatic changes towards warmer and drier conditions (e.g., Zhang et al., 2005; Oroud, 2008; Menzel et al., 2009; Sowers et al., 2011). A large fraction of the renewable water resources in Jordan is generated in the mountainous areas due to the relatively good amount of precipitation falling there compared to the rest of the country. The mountainous region where the average annual precipitation exceeds 200 mm represents ~ 10% of the total area of the country. Detailed calculations by the author of isohyets using GIS indicate that this region receives on average ~32% of the total precipitation falling on the country as a whole, and generates more than 65% of the renewable water resources.

Most watersheds in Jordan suffer from a lack of any type of meteorological and/or hydrological measurements, and where

such measurements exist they are usually of poor quality, and in most cases the flood records do not reflect precipitation events. For instance, the Karak Plateau recorded, on the 22/23 of March, 1991, a significant amount of precipitation ranging from 160 mm in Rabba to 245 mm in the city of Karak, causing a massive flooding in all wadies draining the plateau, yet the average daily discharges of Wadi Mujib, Wadi Karak, Wadi Numera and Wadi Ibin Hammad, for the 23, 24, 25 of March, 1991, as provided by archives of the Ministry of Water and Irrigation, 2001, were 0.038, 0.274, 0.061, and 0.19 m<sup>3</sup>/second, respectively!. Unfortunately, such erroneous "records" are implemented in calibrating models and in planning dams, culverts, and bridges. The deficiency and/or very poor quality of such measurements, in most catchments along with the poor knowledge of the fluvial processes controlling rainfall-runoff dynamics, have led to serious miscalculations of the capacity of dams, bridges and culverts constructed over many catchments in this region. For example, the maximum storage capacity design of both the Wadi Walla and the Wadi Mujib Dams were seriously underestimated, being 8 and 36 million m<sup>3</sup>, respectively. During their operational period, which started around 10 years ago, the volume of overflow during flooding events exceeded the volume of water stored behind them. To reduce the flood water lost from the Wala Dam, the MWI implemented a plan in 2014 to increase the dam's

\* Corresponding author. e-mail: ibrahimoroud@yahoo.com

capacity to 25 M m<sup>3</sup>. In addition to its inadequate design, the Mujib Dam suffers from very serious sedimentation problem ; a study conducted in 2008 by Margane et al. (2008), after only five years of operation, showed that the sediment thickness in some parts of the dam exceeded 14 meters. Such results point to a serious misunderstanding of fluvial processes controlling runoff and sediment production in this environment.

The chronic water shortage in the country along with the increased demands on water resources for the various sectors and to maximize water harvesting, the Jordanian government is planning to construct dams on the main watersheds draining the Karak Plateau. There are four major catchments draining this plateau, Wadi Mujib, Wadi Ibin Hamad, Wadi Karak, and Wadi Numeira. These watersheds suffer from a lack of adequate hydro-meteorological measurement . This being the case, there is an urgent need to adequately assess the water resources potentials there. This assessment is vital for the proper designing and the management of the proposed new dams on these watersheds.

The present paper examines the water budget components of the Numera catchment, which represents typical watershed draining parts of the Karak Plateau. A transient hydrological model with a spatial resolution of one km<sup>2</sup> was run for six continuous years using daily meteorological data collected at nearby meteorological stations operated by the Ministry of Agriculture and the Department of Meteorology, Jordan. Results of this study are operationally important, as they provide the decision makers with realistic estimates of surface runoff and underground recharge, and thus decisions concerning the construction of dams in this watershed or on similar nearby watersheds can be based on scientific grounds rather than on “educated guessing” or poor data records.

**2. Study Area**

The Numera watershed, located around 15 km south of Karak city, covers an area of 100 km<sup>2</sup> and located between latitudes 31.00 and 31.08 degrees North and longitude 35 31 and 35 42 degrees East (Figure 1). The basin may be divided, from a climatological/ topographic perspective, into three zone : The highland (where Mediterranean soil and climate prevail), the middle basin (which represents a transitional zone between the highland and the Jordan Rift), and, finally, the lowland (which is simply part of the Jordan Rift).

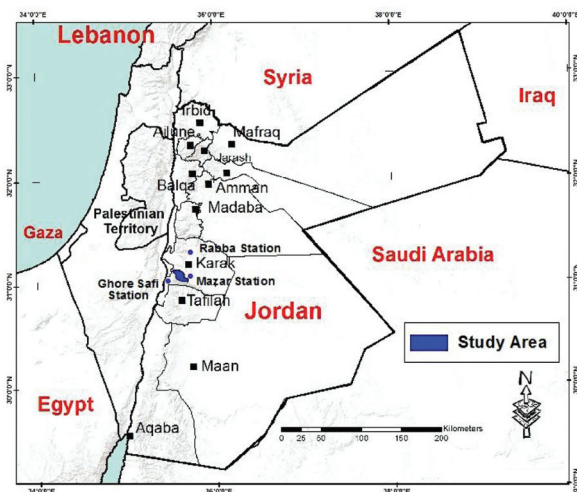


Figure 1. Location of study area.

Figure 2, a digital elevation model obtained from data collected by Aster Satellite with a spatial resolution of 15 m, shows the physiographic setting of the watershed. The basin spans a great relief differentiation, with the elevation ranging from ~ 1300 m above sea level to less than 300 m below sea level. Figure 3 shows the percentage of the area of the basin occupying a given contour interval. The area situated above 600 m represents around 68% of basin, whereas the corresponding value of the areas below 600 m contour line is around 32% only. This indicates that the major portion of the basin is situated in the highlands, and has good water resources potential.

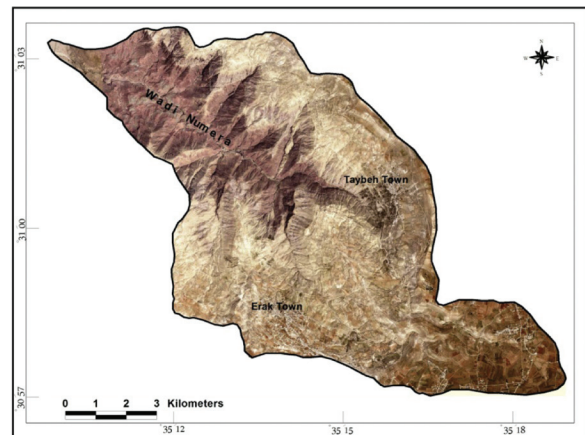


Figure 2. Physiographic and land use patterns of the catchment area.

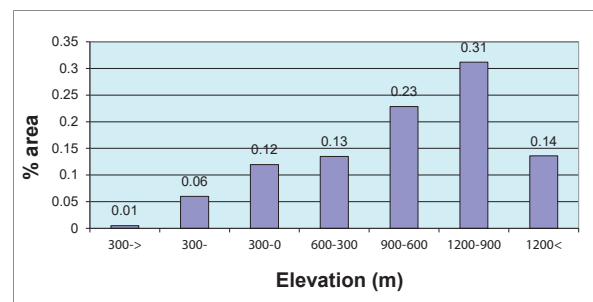


Figure 3. Percentage of area enclosed within 300 m contour intervals.

The highland is composed of Mediterranean red soil which has a good water holding capacity, making it suitable for the cultivation of grains, legumes, summer vegetables and some olive and fruit trees. The middle part of the basin has a yellow soil which reflects the dry conditions prevailing there. Some irrigated agriculture prevails in this part of the basin. The lower reaches of the basin are composed mainly of sandstone with very little soil cover. The basin encompasses a wide range of the climate and vegetation assemblages. The average annual precipitation varies from ~ 310 mm in the highlands where the Mediterranean climate prevails to less than 100 mm in the lower parts near the Dead Sea shoreline. The number of the rainy days with a daily precipitation exceeding 1 mm ranges from ~31 days in the highlands to ~14 days near the Jordan Rift. Substantial inter-annual precipitation variation occurs in this watershed, with a coefficient of variation exceeding 33%. The annual precipitation during the period 1972 through 2014, in a meteorological station situated at the watershed divide in the highlands, varied from a maximum of 560 mm in a very wet year to less than 120 mm in the driest year. This

strong annual precipitation variation is an endemic character of the plateau with adverse consequences on agricultural practices there. Average January daily temperature within the basin ranges from values close to 5 °Celsius in the highlands to more than ~14 °Celsius near the Dead Sea (Oroud, 2011). Subfreezing temperatures occur in the highlands during the cold part of the year, but their occurrence is seldom near the Dead Sea (Oroud, 2007). Being located in a subtropical zone with dominant subsidence, the basin receives an ample amount of solar radiation exceeding 7000 MJ m<sup>-2</sup> year<sup>-1</sup>. The large amount of the annual solar radiation reveals the substantial radiative power available for evapotranspiration processes.

On average, the upper parts of the basin enjoy a Mediterranean-like climate whereas the lower parts experience hyper-arid conditions. The dryness index, which represents the ratio of potential evaporation to average annual precipitation ( $\Theta = P_E/P$ ), varies from 3.5 in the highlands to ~25 in the lower parts of the basin. From an agricultural perspective, rain-fed agriculture could be practiced in areas with a dryness index of less than 5, and controlled grazing in areas with a dryness index between 5 and 10. Areas with a dryness index exceeding 10 are highly fragile to anthropogenic activities, e.g., grazing, with significant adverse consequences on soil erosion and sediment production.

The diversity of terrain, geology, soils, and microclimates had led to intriguing plant assemblages across the basin. Natural vegetation is composed of perennial bushes covering the slopes of the highlands. Low laying bushes are scattered in areas receiving more than 200 mm of annual precipitation. These plant communities are more prevalent on north-facing slopes, where microclimates and soil moisture regimes are more favorable for plant growth. Only drought resistant/evasive xerophytes can survive the very harsh environmental conditions in the lower parts of the basin (Oroud, 2010); patchy plant communities scatter along the washes of wadies and near the shallow ground water where enough moisture penetrates beneath the wadi beds.

The basin has five small settlements located in the upper parts of the basin, with a population close to 7000 inhabitants, and these settlements cover ~ 2% of the basin. Dry-fed agriculture prevails in the upper parts and represents around 33% of the basin. Rangeland with a relatively good native vegetation cover comprises around 15% of the basin. Denuded areas and rocky terrains represent ~ 50% of the basin. There are a few small springs emerging in the middle of the basin, allowing for the cultivation of irrigated crops such as grapes, olives and orchards over limited areas.

### 3. Method of Investigation

The present model integrates the daily surface energy and the soil water balances to simulate precipitation partitioning into evapotranspiration, surface runoff and deep recharge. The water budget of a soil column, where precipitation is the only moisture source, may be expressed in the following form (e.g., Gleick, 1987; McMahon et al., 2013):

$$\frac{\delta S}{\delta t} = P - E_T - R_o - D_p \quad (1)$$

where  $\delta S/\delta t$  is soil moisture change with time,  $P$ ,  $E_T$ ,  $R_o$ , and  $D_p$ , are precipitation, actual evapotranspiration, surface runoff, and deep percolation, respectively, all terms are expressed in  $L/T$ . In arid and semiarid environments, actual evapotranspiration is the largest component on the right hand side of Eq. 1, and as such small errors in this term lead to large absolute errors in the estimates of runoff and deep recharge (e.g., McMahon et al., 2013), and its accurate formulation is quite important. Actual evapotranspiration is either energy-limited or moisture-limited (Alley, 1984; McMahon et al., 2013) and is functionally controlled by available energy, radiative and advective, and soil moisture regime (e.g., Oroud, 2011):

$$E_T = f(P_E, S_m) \quad (2)$$

where  $E_T$  is actual evapotranspiration,  $P_E$  is potential evaporation which is a thermal index, and  $S_m$  is soil moisture availability as influenced by the hydraulic properties of the soil. Potential evapotranspiration is largely controlled by surface net radiation (e.g., Oroud, 2011; McMahon et al., 2013). The energy budget at the surface-atmosphere boundary may be expressed in the following form (e.g., Oroud, 1999; Oroud, 2011):

$$Rn = S(1 - \alpha_s) + L_{\downarrow} - L_{\uparrow} \quad (3)$$

where  $Rn$ ,  $S$ ,  $\alpha_s$ , are net radiation, global radiation, surface albedo, incoming atmospheric and emitted surface long wave radiation ( $Wm^{-2}$ ), respectively. Eq. 3 represents the radiative component of the atmospheric forcings determining potential evapotranspiration (McMahon et al., 2013). The various terms which influence net radiation are solar radiation absorption, incoming long wave atmospheric radiation and emitted surface radiation. These terms were calculated from observed and interpolated meteorological elements obtained from the nearby meteorological stations.

Solar radiation is estimated from sunshine hours and extraterrestrial radiation at the top of the atmosphere. Extraterrestrial solar radiation ( $s_{ext}$ ) over a flat surface is determined by solar declination and geographic latitude (Iqbal, 1983):

$$S_{ext} = \int_{sr}^{ss} Go dt \quad (4)$$

where  $Go$  is the solar radiation reaching the top of atmosphere at a given latitude (see Iqbal, 1983),  $sr$  and  $ss$  are sunrise and sunset, respectively. Global solar radiation is calculated for each resolution cell using the following form (Iqbal, 1983):

$$S = S_{ext} (\mu_o + \gamma \frac{n}{N}) \quad (5)$$

where  $S$  is daily global solar radiation,  $\mu_o$  is the fraction of extraterrestrial solar radiation reaching the surface during overcast conditions,  $g$  is the slope of the regression line linking surface solar radiation to sunshine hours,  $n$  and  $N$  are actual sunshine hours and theoretical daylight length, respectively. The values of  $\mu_o$  and  $g$  are widely reported to be 0.25 and 0.5, respectively (e.g., Iqbal, 1983; Allen et al., 1998). Solar radiation correction for the elevation difference in the catchment was introduced after Allen et al. (1998).

Atmospheric radiation is calculated using the formulation presented by Brutsaert (1982):

$$L_{\downarrow} = \varepsilon_a \sigma T_a^4 \quad (6)$$

where  $T_a$  is near surface air temperature (K),  $\epsilon_a$  is atmospheric emissivity which is determined primarily by water vapor concentration in the lower troposphere (e.g., Oroud and Nasserallah, 1998). Atmospheric emissivity ranges from values close to 0.72 in a relatively dry cold atmosphere similar to clear cold winter nights in Jordan to more than 0.95 during overcast conditions with low level clouds. Emitted surface radiation is determined primarily by surface temperature and the level of surface moisture; surface emissivity ranges from ~0.94 for dry soils to 0.97 for wet soils. Surface albedo and surface emissivity were assumed to be 0.23, and 0.96, respectively.

The soil fabric in each resolution cell is assumed to be comprised of two compartments, a relatively thin layer at the top and a deep layer. The top layer is assumed to hold 0.2 of water stored in the entire soil profile, and this assumption is consistent with the US Geological Survey Curve Number assumptions (e.g., Solomon and Cordery, 1984; Dingman, 1992; Nishat et al., 2007; Moroizumi et al., 2009). This depth also provides an adequate assessment of actual evapotranspiration from the soil profile (e.g., Romano and Giudici, 2009). Actual evapotranspiration from the soil is calculated using the following form (e.g., Liu and Smedt, 2004):

$$E_T = \begin{cases} P_E, P \geq P_E \\ (P - P_E) \left( \frac{m_1 - \lambda}{F_{c1} - \lambda} \right)^3 + (P_E - \beta) \frac{(m_2 - w_{p2})}{(F_{c1} - w_{p1} + F_{c2} - w_{p2})}, P < P_E \end{cases} \quad (7)$$

where  $P_E$  is potential evapotranspiration,  $m_1$  and  $m_2$  are upper and lower layers moisture,  $\lambda$  is air dry soil moisture, and  $\beta$  is evapotranspiration from the first layer,  $F_{c1}$  and  $F_{c2}$  are field capacity of upper and lower soil layers,  $w_{p1}$  and  $w_{p2}$  are wilting points for layers 1 and 2. Potential evapotranspiration is calculated using the Penman method as modified by Allen et al. (1998); this formulation accounts for the radiative (net radiation) and advective (wind speed, surface roughness, and vapor pressure deficit) components. In this formulation, evapotranspiration takes place from the top layer only when this layer is at field capacity, but abstraction from the lower layer occurs when atmospheric demands are not met from the first layer. In Eq. 7, evaporation and transpiration proceed from the top layer, whereas only transpiration occurs from the second deeper layer. The first layer has limited plant available moisture, and therefore the water loss from this layer is determined primarily by soil evaporation. It is well-known that the soil evaporation decreases non-linearly as soil water content decreases (e.g., Ritchie, 1972; Alley, 1984; Liu and Smedt, 2004; McMahon et al., 2013). To make the parameterization consistent with plant phenology, it is assumed that transpiration for areas situated above 700 m occurs during the period, end of January through end of June. This assumption is consistent with field crops grown in this area which usually start to emerge and develop after the end of January in the highlands in the eastern Mediterranean due to the cold temperatures there (e.g., Oroud, 2012).

Surface runoff and deep recharge are calculated using a bucket method such that when the first layer reaches its field capacity, excess water there is drained to the deeper layer. Excess water in the deeper layer beyond field capacity is assumed to be lost as deep recharge. This occurs when the two

soil layers reach their field capacities. Runoff occurs when daily precipitation exceeds soil saturation of the top layer and a retention parameter (e.g., Nishat et al., 2007; Moroizumi et al., 2009):

$$\begin{aligned} Ro &> 0 : P > (\theta_{s1} + \psi) \\ Ro &= 0, \text{ otherwise} \end{aligned} \quad (8)$$

where  $Ro$  is surface runoff,  $\theta_{s1}$  is soil layer saturation,  $\psi$  is a retention parameter which accounts for rainwater trapped in surface irregularities and micro reliefs.

It is assumed in this formulation that snow occurs when the average daily air temperature of a resolution cell is 3 °C or less (e.g., Dingman, 1992). The mass of melted snow is a complex function of daily solar radiation, conduction from the underlying ground, sensible heat flux exchange due to turbulent mixing, atmospheric humidity, and downward long wave radiation from cloud cover, particularly low clouds (e.g., Dingman, 1992; Oroud and Nasserallah, 1998). Due to the complexity of the snow melting processes, the widely used degree day method (e.g., Solomon and Cordery, 1984; Liu and De Smedt, 2004) is employed in the present paper. This parameterization is expected to be confined to the highland, as precipitation in the form of snow does not usually occur below 700 m in this basin.

### 3. Model Input

The various physical properties such as hydraulic properties of soil, grid slope, land cover/ use, and climate gradient were extracted from field surveys, topographic maps, remote sensing images, and GIS tools. Soil characterizations – in terms of soil thickness, porosity, field capacity, wilting point, and air dry properties – were deduced from field surveys, soil maps, and physiognomy of each resolution cell. Average soil properties of each cell were tabulated using soil and topographic maps. Soil porosity ranges from 0.46 for clay like soils to around 0.43 for sandy like soils (e.g., Nimo, 1984). Field capacity for the clayey soils in the mountainous areas, where relatively deep Mediterranean soils dominate, is around 0.36 and wilting point is ~ 0.24; corresponding values for sand like soil are 0.14 and 0.06, respectively. These values are consistent with values reported for this type of soil in this environment (Dingman, 1992). The influence of slope on the soil hydraulic properties was taken into account when calculating the effective holding capacity such that effective holding capacity decreases as slope increases beyond a given threshold level.

The catchment does not have any hydrological or meteorological stations, and thus meteorological data observed in the nearby locations were employed to generate the needed atmospheric data to calculate the energy and water balance components of each resolution grid. Precipitation is obtained from daily measurements observed in the southern Mazar station, located near the watershed divide in the highlands. The upper portions of this watershed experiences climatic conditions similar to those prevailing over the station. Precipitation series observed in this station were cross correlated with corresponding values observed at Rabba station, a first class meteorological station located about 20 km north of the catchment area and operated by the Department

of Meteorology, Jordan. A good correlation was obtained and missing data at Mazar station were filled using the regression method. Precipitation falling on each grid could be obtained using a variety of methods, such as the Inverse Distance, the Krigging or the Contour Line (e.g., Dingman, 1992). Due to the steep elevation gradient, the Contour Line would be the most suitable interpolation method because of the steep precipitation gradient across the basin. Precipitation data for a station located at the highland and another one situated near the southern end of the Dead Sea were employed to extrapolate precipitation at each resolution grid. As an independent check, the assemblages of natural vegetation and land use patterns were utilized as a proxy indicator of the precipitation gradient.

Daily meteorological data gathered at Rabba meteorological station were implemented to extrapolate solar radiation, air temperature, atmospheric water vapor pressure, wind speed, and cloud cover after taking into account average elevation of each cell. Air temperature gradient between the mountainous station located at 920 m and the one near the southern edge of the Dead Sea (-350 m) was found to range from 0.006 °C/m in January to about 0.007 °C/m in July. This temperature gradient is commensurate with the widely documented environmental lapse rate of 0.0065 °C/m observed in the lower troposphere. Ambient vapor pressure depends strongly on air temperature (e.g., Allen et al., 1998). Figure 4 shows the linkage between the average monthly air temperature and the average monthly actual vapor pressure for two stations situated near the drainage basin, one in the mountains and the other near the Dead Sea. Given this strong linkage, the actual vapor pressure for each cell is determined using the following expression (Oroud, 1998):

$$e_a(j,i) = e_a + \frac{\partial e}{\partial T} \frac{\partial T}{\partial z} \delta z \quad (9)$$

where  $e_a(j,i)$  is actual vapor pressure of cell  $j,i$ ,  $e_a$  is the observed actual vapor pressure at the meteorological station, and  $\delta z$  is elevation difference between the meteorological station and the intended cell. It is widely known that ambient water vapor pressure is closely linked to near surface air temperature.

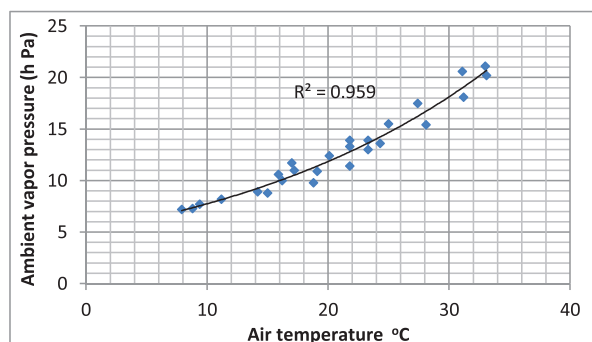


**Figure 4.** Linkage between average monthly air temperature and average monthly actual vapor pressure for two stations situated near the drainage basin.

**5. Model Results**

The simulated daily solar radiation in the highlands ranged from 10.2 MJ m<sup>-2</sup> in December to 30.6 MJ m<sup>-2</sup> in June, respectively. The corresponding simulated values for the lower parts of the basin near the Dead Sea were 10.6 and

28 MJ m<sup>-2</sup> day<sup>-1</sup> in December and June, respectively. Global solar radiation observed by the author in the mountainous area during December and June, 2010 were 9.8 and 29.9 MJ m<sup>-2</sup> day, respectively. Figure 5.a shows a typical diurnal solar radiation regime in the mountainous areas near the watershed divide during June. Likewise, the long term observed daily solar radiation reaching the Dead Sea area in December and June were reported to be 10 and 27.5 MJ m<sup>-2</sup>.day<sup>-1</sup>, respectively (Hecht and Gertman, 2003). These results lend a strong support to the adequacy of the input values for the model. Figure 5.b shows the spatial distribution of simulated solar radiation reaching the watershed during December.

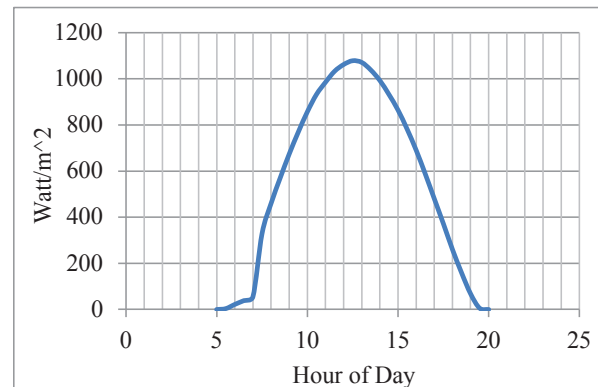


**Figure 5.a.** A typical diurnal solar radiation regime in the mountainous areas as observed by author during June. The slight dip in the early morning hour is due to the obstruction of sun by an obstacle.

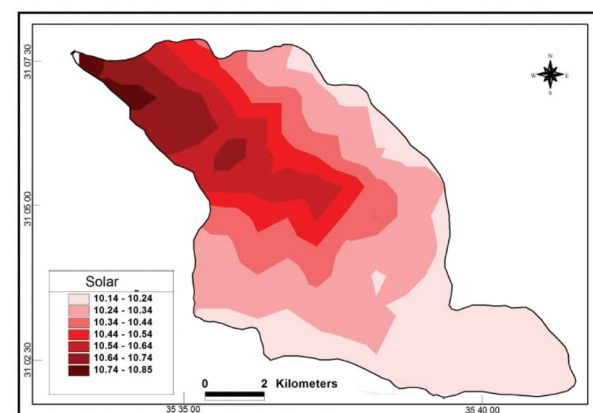


**Figure 5.b.** Simulated daily solar radiation during December (MJ m<sup>-2</sup>. day<sup>-1</sup>).

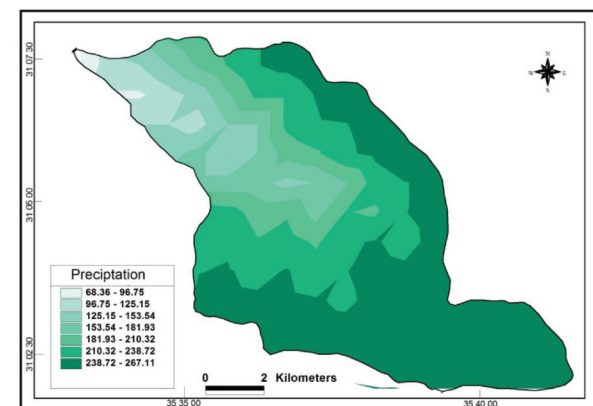


**Figure 6.** Spatial distribution of average annual precipitation across the basin.

Annual precipitation is characterized by a steep gradient across the watershed, ranging from 270 mm in the highlands to about 70 mm in the lower portions during the simulation period (Figure 6).

During the six-year period, the average annual areal precipitation falling on the basin as a whole was around 26 million m<sup>3</sup>. Annual potential 1750 mm in the lower reaches of the basin (Figure 7).

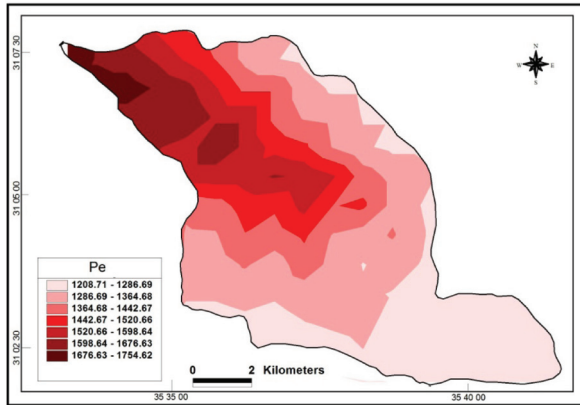


**Figure 7.** Potential evapotranspiration across the basin during December through end of March.

Of special importance is the evaporative power of the contiguous atmosphere during the period of December through the end of March, as more than 80% of precipitation falls during this time. During this period, PE ranges from ~185 mm in the mountainous areas to ~330 mm in the lower reaches of the basin. Figure 8 shows the spatial distribution of average actual evapotranspiration (AE) during the cold part of the year, December through the end of March. During this time of year, AT ranges from 70 mm in the lower part of the basin to about 130 mm in the highlands. The ratio of AT to precipitation during the cold part of the year ranges from figures close to 100% in the lower parts to about 65%-70% in the highlands. The meager amount of precipitation along with the significant evaporative power in the lower parts is responsible for the total loss of precipitation by direct evaporation.

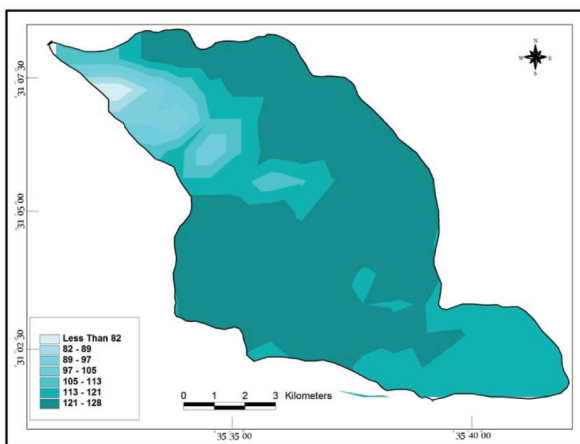


**Figure 8.** Actual evapotranspiration across the basin during December through end of March.

Runoff displays a substantial spatial heterogeneity across the basin, ranging from 55 mm over steep terrains to zero near the Dead Sea shoreline (Figure 9). A significant runoff occurs over steep slopes where the surface is devoid of vegetation and the soil is relatively thin. Runoff in semiarid areas has been reported to represent a significant fraction of annual precipitation, particularly for bare, low storage surfaces (e.g., Lal, 1991).

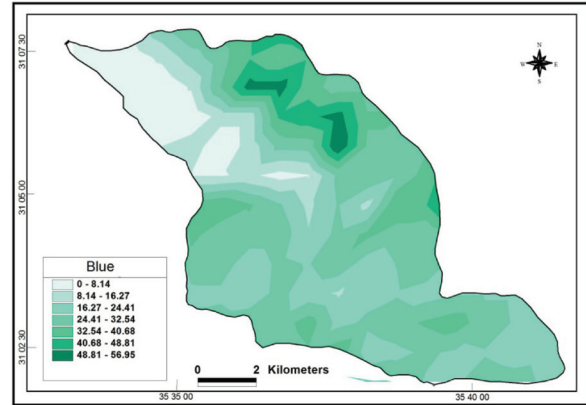


**Figure 9.** Spatial distribution of average runoff during six year the simulation period.

Relatively, little runoff is generated in the water divide as a result of the deep soils and the gentle slope there. Deep soils are characterized with a large water holding capacity which would explain the suitability of flat/ gentle sloping terrains in the watershed divide to agricultural practices, as large fractions of precipitation are stored in the deep soil profile and being subsequently consumed in plant transpiration (e.g., Al Qudah, 2001). The annual runoff generated in this catchment during the six-year simulation period was close to 2.0 million m<sup>3</sup>. This catchment produces relatively little deep underground recharge which varies from less than 30 mm year<sup>-1</sup> in limited areas in the highlands to almost zero in the lower reaches. Almost all the areas located below the 600 m contour line have a negligible contribution to underground recharge due to the scanty amount of precipitation and the high evaporative power of the contiguous atmosphere (Figure 10). Scanty precipitation events tend to wet a shallow soil layer which is subsequently lost to the contiguous atmosphere via direct evaporation, with little or absent contribution to runoff and underground recharge. The simulated underground recharge for the whole catchment, as delineated by its topographic water divide, is around 1.25 million m<sup>3</sup>. The total blue water fluxes for the basin as a whole during the six-year period represented around 12.5% of areal precipitation. This ratio is consistent with those obtained in catchments situated in similar environments (e.g., Margane et al., 2005; Al Kuisi and El-Naqa, 2013; Schulz et al., 2013).

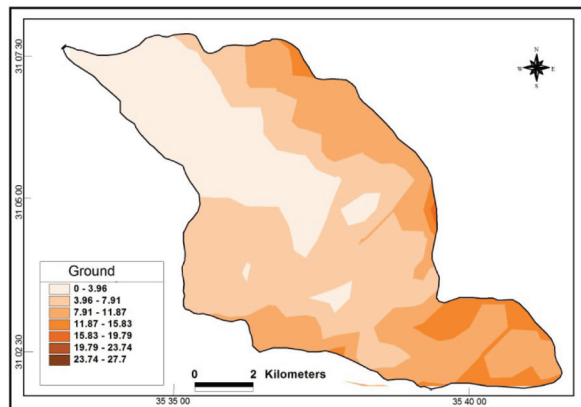


**Figure 10.** Spatial distribution of simulated underground recharge during the six year period.

## 6. Field measurements

The data compiled by the Ministry of Water and Irrigation (2012) for the period January, 1, 1990 through January, 31, 2010 indicate that the Numera Wadi, which drains the investigated catchment area, has an average water flow, including flooding, of  $\sim 1.53$  Million  $m^3$  per annum. Furthermore, a field campaign carried out by the author during Jul, 2013 indicated that the water emerging from the springs in the catchments was  $\sim 800$  thousand  $m^3$ . Thus, total annual blue water fluxes from the catchment was around 2.3 million  $m^3$  during the simulation period. The measured annual flow appears to be less than the simulated blue water yield by about one million  $m^3$ . Several reasons are responsible for this incongruity. In pars, measurements by the MWI are frequently faulty, as days with heavy precipitation as recorded in meteorological stations did not reflect any flooding event. Such records tend to underestimate actual blue water fluxes. In addition, measurements of spring discharges were carried out in mid-summer, and thus measured flow is expected to be less than the sum over all months, as discharge from springs increases in winter and spring following rainy periods. Discharges from some springs were not measured and this has contributed to the discrepancy. Additionally, some water generated in the watershed is likely seeping directly to the Dead Sea, and this part is not accounted for. Despite this difference, simulated results are in line with previous studies carried out in similar catchments (e.g., Margane et al., 2005; Schultz et al., 2013).

## 7. Discussion and Conclusion

The Numera watershed represents a typical catchment in the Karak Plateau, and its water budget components are not expected to deviate appreciably from other catchments in the Plateau. Calculations show that the ratio of actual evapotranspiration for the catchment as a whole is around 87.5% of areal precipitation. Deep recharge occurs primarily in the highlands, and this is clearly confirmed by the abundance of the emerging springs in the areas located between 800- 900 m above mean sea level. It should be indicated that during the six-year simulation period, precipitation was less than the long term average by about 15% which means that blue water fluxes should have been larger than what is reported in the present paper. The elasticity of blue water fluxes to

precipitation variations in this environment is quite large (e.g., Oroud, 2008; Yang and Yang, 2011). The results obtained in the present paper are congruent with previous studies conducted in catchments situated in different parts of Jordan. In a study to assess deep recharge and underground water susceptibility to pollution in the Lajune area, midway between Karak city and the desert highway near Qatraneh, Margane et al. (2005) indicated that the underground recharge varies from  $\sim 10$  mm year<sup>-1</sup> in the drier realms to  $\sim 20$  mm year<sup>-1</sup> in the less drier locations in the west and southwest of the catchment, which constitute  $\sim 4\%$  to  $9\%$  of areal precipitation. Further, Schulz et al. (2013) indicated that the average annual underground recharge for the Amman-Zarqa underground basin is around 105 million  $m^3$  ( $\sim 21$  mm year<sup>-1</sup>) which represents around 9.5% of areal precipitation over the catchment. The ratio of the underground recharge increases in the more humid areas of the country; Hobler et al, (2001) estimated the underground recharge ratios for areas close to Ajlune and Salt cities, where the average annual precipitations in the range 600 - 550 mm are around 21.4% and 18.2% of annual precipitation, respectively. Blue water fluxes, both surface runoff and deep underground recharge, become insignificant, being less than 2%, in arid catchments in this region (e.g., Al Kuisi and El-Naqa, 2013); this is the case for the lower parts of the Numera basin, as shown in Figures 9 and 10, where the surface runoff and deep recharge are close to zero.

It has been shown that the deep soils in this catchment contribute less blue water than the thin soils or rocky terrains. As soil depth increases in this environment, a larger fraction of precipitation is stored in the soil fabric which is subsequently lost via transpiration (green water) rather than being partitioned via surface runoff and/or deep recharge. These results are consistent with field observations and simulations results carried out in similar environments (e.g., Bellot et al., 2001; Farmer et al., 2003; Ranjan et al., 2006; Seyfried and Wilcox, 2006), and ascertain the very delicate nature of runoff and deep recharge in these catchments (e.g., Alley, 1984).

An important outcome of this study is the pronounced disparity of surface runoff across the catchment with a significant runoff occurring over steep terrains in the highlands. Field surveys show that these slopes are highly dissected with numerous deep arroyos. These dissected landscapes and the wide spread of rills and gullies reveal the substantial erosional potentials over these slopes. Consequently, extra care must be exercised when constructing dams over these watersheds, as large volumes of sediments are produced, leading to severe shortening of life spans of these dams. An obvious example is the accumulation of large volumes of sediments in the Mujib Dam which gets a large portion of its water supply from the Karak Plateau. A joint Jordanian-German study conducted in 2008, only five years following the dam construction, indicated that the thickness of sediments in the Mujib Dam was in excess of 14 m in some parts of the dam (MWI, 2008). This result points out to serious misunderstandings of the fluvial processes controlling rainfall-runoff/sediment production in this environment. The implication of this finding is that erosion control over these catchments must be a mandatory step before any dam construction. Pioneering

geomorphological studies (e.g., Langbein and Schum, 1958; Collins and Bras, 2008) have shown that the sediment yield reaches its maximum in areas receiving between 250- 300 mm of annual precipitation, decreasing sharply on both sides of this maximum, in the lower end owing to a deficiency of runoff and in the other to increased vegetation density. In fact, most important watersheds in Jordan are situated in this precipitation zone where the vegetation cover is quite sparse or even absent and soils are poorly managed. Thus, soil erosion management in these watersheds must be given an extra attention prior to constructing dams in this highly fragile environment.

The present model could be linked with an erosion model to delineate areas with serious erosional potentials that need to be managed adequately prior to dam construction. Results of the present study should be regarded as a first step in evaluating blue water fluxes from these catchments, and meteorological, hydrological, and geomorphological measurements need to be established in these watersheds to build a reliable data base to understand the linkage between rainfall - runoff/ sediment yield in this highly water stressed region.

## References

- [1] Al Kuisi, M., El-Naqa, A., 2013, GIS based spatial groundwater recharge estimation in the Jafr basin, Jordan- application of wetSpss models for arid region, *Revista Mexicana de Ciencia Geologica* (in press),
- [2] Al Qudah, B., 2001, Soils of Jordan, in: Zdruli et al. (eds.), *Soil Resources of Southern and Eastern Mediterranean Countries*, Bari: CIHEAM, pp 127-141.
- [3] Allen, R. G., Pereira, L. S., Raes, D., Smith, M., 1998. *Crop Evapotranspiration Guidelines for Computing Crop Water Requirements*, FAO Irrigation and Drainage Paper 56, FAO, Rome.
- [4] Alley, W., 1984, on the treatment of evapotranspiration, soil moisture accounting, and aquifer recharge in monthly water balance models, *Water Resour. Res.*, 20, 1137-1149.
- [5] Belloc, J., Bonet, A., Sanchez, J., Chirino, E., 2001, Likely effects of land use changes on the runoff and aquifer recharge in a semiarid landscape using a hydrological model, *Landscape and Urban Planning*, 55, 41–53
- [6] Brutsaert, W., 1982. *Evaporation into the Atmosphere*, Reidel Pub. Co., Dordrecht.
- [7] Collins, D. B., Bras, R. L., 2008, Climatic control of sediment yield in dry lands following climate and land cover change, *Water Resources Research*, 44, CiteID W10405.
- [8] Dingman, S. L., 1992, *Physical Hydrology*, Prentice Hall.
- [9] Farmer D, Sivapalan M, Jothityangkoon C., 2003. Climate, soil, and vegetation controls upon the variability of water balance in temperate and semiarid landscapes: downward approach to water balance analysis. *Water Resources Research* 39: 1035.
- [10] Gleick, P.H., 1987, Regional hydrologic consequences of increases in atmospheric Carbon Dioxide and other trace gases, *Climatic Change* 10(2):137-161.
- [11] Hecht, A., Gertman, I., 2003, Dead Sea meteorological climate, in: Nevo, E., Oren, A., Wasser, S., eds. *Fungal Life in the dead Sea*, 69-116.
- [12] Hobler M, Margane A, Almomani M, Subah A (2001) Contributions to the hydrogeology of Northern Jordan. Ministry of Water and Irrigation (MWI) and Federal Institute for Geosciences and Natural Resources (BGR). Report Vol. 4. In: *Groundwater Resources of Northern Jordan*
- [13] Iqbal, M., 1983. *An Introduction to Solar Radiation*. Academic Press, New York.
- [14] Lal R., 1991, Current research on crop water balance and implications for the future. In: Sivakumar MVK, Wallace JS, Renard C, Giroux C (Editors), *Soil water balance in the Sudano-Sahelian Zone*, Proceedings of an International Workshop, Niamey, Niger. IAHS Press. Inst. Hydrol. Wallingford, UK pp. 31-44.
- [15] Langbein, W. B., Schum, S. A., 1958, Yield of sediment in relation to mean annual precipitation, *Transactions, American Geophysical Union*, Volume 39, Issue 6, p. 1076-1084
- [16] Liu, Y. B., De Smedt, F., 2004, *A GIS-based Hydrological Model for Flood Prediction and Watershed management*, Dept. Hydrology and Hydraulic Engineering, Vrije Univ. Brussel, Belgium.
- [17] Margane, A., Borgstedt, A., Subah, A., Hajali, Z., Almomani, T., Hamdan, I., 2008, Delineation of Surface Water Protection Zones for the Mujib Dam, Technical Report No. 10, 132 pp.
- [18] Margane, A., Subah, A., Khalifa, N., Almomani, T., Ouran, S., Hajali, Z., Jaber, A., Atrash, A., Hijazi, H., Tarawneh, R., 2005, Mapping of Groundwater Vulnerability and Hazards to Groundwater in the Karak – Lajjun Area Federal Institute for Geosciences and Natural Resources (BGR), Ministry of Water and Irrigation (MWI) Groundwater Resources Management Project 5.

- [19] McMahon, T. A., Peel, M. C., Lowe, L., Srikanthan, R., and McVicar, T. R., 2013, Estimating actual, potential, reference crop and pan evaporation using standard meteorological data: a pragmatic synthesis, *Hydrol. Earth Syst. Sci.*, 17, 1331–1363, doi:10.5194/hess-17-1331.
- [20] Menzel, L., Koch, J., Onigkeit, J., Schaldach, R., 2009, Modeling the effects of land-use and land cover change on water availability in the Jordan river region, *Advances Geosc.*, 21, 73-80.
- [21] Ministry of Water and Irrigation (Jordan), 2001, Ground Water Management Plan for the Amman- Zarqa Basin Highlands, 64 pp.
- [22] Ministry of Water and irrigation (Jordan), 2012, Unpublished reports.
- [23] Morozumi, T., Hamada, H., Sukchan, S., Ikemoto, M., 2009. Soil water content and water balance in rain-fed fields in North East Thailand, *Agric. Water Manage.* 96, 160-166.
- [24] Nimmo, G. R., 2004, Porosity and pore distribution, in Hillel, D., ed. *Encyclopedia of Soils in the Environment*, London, Elsevier, Vol. 3, 295-303.
- [25] Nishat, S., Guo, Y., Baetz, B. W., 2007. Development of a simplified continuous simulation model for investigating long term soil moisture, *Agric. Water Manage.* 92, 53-63.
- [26] Oroud, I. M., 1998, The influence of heat conduction on evaporation from sunken pans in hot, dry environments. *Journal of Hydrology*, 210, 1-10.
- [27] Oroud, I. M., 2001, A new formulation of evaporation temperature dynamics of saline solutions, *Water Resources Research*, 37, No. (10), 2513-2520.
- [28] Oroud, I. M., 2007, Spatial and temporal distribution of frost in Jordan: *The Arab World Geographer*, 10, (2) 82-91.
- [29] Oroud, I. M., 2008, The impact of climate change on water resources in Jordan: in: Zerieni, F. and Hotzl, H. (Eds.), *Climatic Changes and Water Resources in the Middle East and North Africa*, pp 109-124, Springer.
- [30] Oroud, I. M., 2011, Evaporation from the Dead Sea and its implications on its water balance, *Theoretical and Applied Climatology*, DOI 10.1007/S00704-0452-6.
- [31] Oroud, I. M., 2012, Climate change impact on green water fluxes in the eastern Mediterranean.: pp 3-15 In: Leal Filho, W. (ed) "Climate Change and the Sustainable Management of Water Resources", Springer, DOI 10.1007/978-3-642-22266-5.
- [32] Oroud, I. M., and H. Nasrallah, 1998, Incoming long-wave radiation enhancement by cloud cover. *Physical Geography*, 19, no. 3, 256- 270.
- [33] Oroud, I. M., 2010, "Climate: Dry." In: *Encyclopedia of Geography*. SAGE Publications. <[http://www.sage-ereference.com/geography/Article\\_n170.html](http://www.sage-ereference.com/geography/Article_n170.html)>.
- [34] Oroud, I. M., 1999, Temperature and Evaporation dynamics of saline solutions. *Journal of Hydrology*, 226, 1-10.
- [35] Ranjan, S., Sawamoto, So., Sawamoto, M., 2006, Effects of climate and land use changes on groundwater resources in coastal aquifers, *Journal of Environmental Management*, 80, 25–35.
- [36] Ritchie, J., 1972. Model for predicting evaporation from a row crop with incomplete cover, *Water Resour. Res.* 8, 1204-1213.
- [37] Romano, E., Giudici, M., 2009, on the use of meteorological data to assess evaporation from a bare soil, *J. Hydrol.*, 372, 30-40. Doi: 10.1016/j.jhydrol.2009.04.003.
- [38] Schulz, S., Siebert, C., Rödiger, T., Al-Raggad, M., Merz, R., 2013, Application of the water balance model J2000 to estimate groundwater recharge in a semi-arid environment: a case study in the Zarqa River catchment, NW-Jordan, *Environmental Earth Sciences*, 69, 605-615
- [39] Seyfried , M., Wilcox, B., 2006, Soil water storage and rooting depth: key factors controlling recharge on rangelands, *Hydrological Process, Hydrological Processes*, 20, 3261–3275, DOI: 10.1002/hyp.6331
- [40] Solomon, S. I., Cordery, I., 1984, *Hydrometeorology*, WMO-No. 364.
- [41] Sowers, J., Vengosh, A., Weinthal, E., 2011, Climate change, water resources, and the politics of adaptation in the Middle East and North Africa, *Climatic Change*, 104:599–627, DOI 10.1007/s10584-010-9835-4
- [42] Yang, H., Yang D., 2011, Derivation of climate elasticity of runoff to assess the effects of climate change on annual runoff, *Water Resources Research*, 47, W07526, doi:10.1029/2010WR009287, 2011
- [43] Zhang, X., Aguilar, E., Sensoy, S., Melkonwan, H., Tagiyeva, U., Ahmad, N., Kutaladze, N., Rahimzadeh, F., Taghipour, A., Hantosh, T.H., Albert, P., Semawi, M., Ali, M.K., Al-Shabibi, M.H.S., Al-Oulan, Z., Zatarí, T., Khelet, I.A., Hamoud, S., Sagir, R., Demircan, M., Eken, M., Adiguzel, M., Alexander, L., Peterson, T.C. & Wallis, T., 2005, Trends in Middle East climate extremes indices from 1950 to 2003. *J. Geophys. Res.* 110.